Nonlinear dynamics of the director of a nematic crystal in a magnetic field

V. G. Kamenskiĭ

L. D. Landau Institute of Theoretical Physics, Academy of Sciences of the USSR
(Submitted 28 April 1984)
Zh. Eksp. Teor. Fiz. **87**, 1262–1276 (October 1984)

The dynamics of the director of a nematic liquid crystal in a constant magnetic field is considered. It is shown that, for certain values of the parameters of the system, an external excitation (pulsed magnetic field) can produce soliton solutions in the system. These solutions are localized in narrow spatial regions in which the angle of deviation of the director from the equilibrium position varies between zero and π. The parameters of these solitons are found as functions of initial excitation and of the parameters of the system. Possible experimental verification of these results is examined.

I. INTRODUCTION

The nonlinear dynamics of liquid crystals has recently begun to be intensively investigated. Current interest in this problem is due to a number of factors. Above all, it is due to the further development of the theory of the liquid-crystal state, which is now complete for phenomena that have a solution in the linear approximation. The other factor governing the importance of such studies is the experimental data obtained in recent years in a number of laboratories, which cannot be explained by linear theory. Finally, studies of nonlinear phenomena in liquid crystals are promising from the point of view of searches for new technological applications.

A large number of liquid crystals with appreciably different physical properties has now been synthesized. The wide range of variation of their characteristic parameters, and the relative simplicity of experiments in which such crystals are investigated, make them a unique object for the investigation of nonlinear phenomena.

In this paper we investigate the dynamics of the director of a nematic liquid crystal in a magnetic field. This problem has been examined in the linear approximation by a number of authors, and the results are well known (see Refs. 1 and 2 and the literature cited therein). However, in view of the considerable complexity of the equations describing the dynamics of nematic liquid crystals, all previous work has been virtually confined to the study of small deviations of the director from the equilibrium position.

A numerical calculation was used in Ref. 3 to investigate the high-frequency dynamics of the director of a nematic crystal in a magnetic field. However, this analysis was confined to uniform motion, i.e., space effects were not discussed. On the other hand, it is interesting to consider the dynamics of the director with allowance for spatial relationships, especially since there are experimental indications that such effects are important. The propagation of director waves due to uniform shear flow in a nematic liquid crystal was investigated experimentally in Ref. 4. It was found that the distribution of the director motion orientation takes the form of a sequence of regions with perpendicular alignment. The qualitative theory[5] constructed to describe these experimental results explains the appearance of soliton solutions in the propagation of the director wave. This explanation seems to be completely acceptable.

The essential point is that the orientation of the director in liquid crystals is directly related to the optical properties of the medium, so that its distribution can be directly observed experimentally.

The problem that we have posed is very topical in view of the foregoing.

II. EQUATIONS OF MOTION

Consider a homeotropic layer of a nematic crystal with one free surface. The layer is placed in a constant magnetic field **H** perpendicular to it. We shall suppose, in addition, that the bonding of the molecules to the substrate is weak, i.e., the boundary has no effect on the orientation of the director, or affects it only in a narrow layer.

The equations describing the dynamics of nematic liquid crystals, obtained by Ericksen and Leslie,[6] are well known. The equation of motion of the director **n** can be written in the following form:

$$J\frac{d}{dt}\left[\mathbf{n}\times\frac{d\mathbf{n}}{dt}\right]=[\mathbf{n}\times\mathbf{h}]-[\mathbf{n}\times\mathbf{R}], \tag{1}$$

where J is the density of the moment of inertia, **h** is the body force producing the equilibrium value of **n**, and **R** is the dissipative force. The director has the property $\mathbf{n}^2 = 1$ and all its variations are rotations.

The forces **h** and **R** are given by[1]

$$\begin{gathered}\mathbf{h}=K_1\nabla(\operatorname{div}\mathbf{n})-K_2\{(\mathbf{n}\operatorname{rot}\mathbf{n})\operatorname{rot}\mathbf{n}\\+\operatorname{rot}(\mathbf{n}(\mathbf{n}\operatorname{rot}\mathbf{n}))\}+K_3\{\operatorname{rot}[\mathbf{n}\times[\mathbf{n}\times\operatorname{rot}\mathbf{n}]]\\-[\operatorname{rot}\mathbf{n}\times[\mathbf{n}\times\operatorname{rot}\mathbf{n}]]\}+\chi_a(\mathbf{Hn})\mathbf{H},\\R_i=\gamma_1N_i+\gamma_2n_jA_{ji},\end{gathered} \tag{2}$$

where

$$A_{ij}=\frac{1}{2}\left(\frac{\partial v_i}{\partial x_j}+\frac{\partial v_j}{\partial x_i}\right),\qquad \mathbf{N}=\frac{d\mathbf{n}}{dt}-\frac{1}{2}[\operatorname{rot}\mathbf{v}\times\mathbf{n}],$$

v is the velocity of the material, γ_1 and γ_2 are the viscosity

 0038-5646/84/100723-09$04.00

coefficients, K_a are Frank constants, and χ_a is the anisotropic part of the magnetic susceptibility. The solution of (1) is quite difficult in arbitrary geometry because the deviation of the director from the position of equilibrium (along the field $\mathbf{H}$) produces the motion of the mass of the crystal with nonzero gradient and this, in turn, affects the motion of the director. Allowance for this so-called reverse-flow effect can be made in special cases but complicates calculations quite substantially. There is, however, one geometry in which the reverse flow is absent (pure torsion), and we shall confine our analysis to this case. It is illustrated in Fig. 1.

The equation of motion of the director $\mathbf{n} = (0, \sin\vartheta, \cos\vartheta)$ is reduced in this case to the well-known sine-Gordon equation

$$J\frac{\partial^2\varphi}{\partial t^2} - K_2\frac{\partial^2\varphi}{\partial x^2} + \gamma_1\frac{\partial\varphi}{dt} + \chi_a H^2 \sin\varphi = 0, \tag{3}$$

where $\varphi = 2\vartheta$. We note that the choice $\mathbf{H}\|z$ is not essential to obtain this equation. For $\mathbf{H} = (0, \sin\psi, \cos\psi)$ lying in the zy plane, the equation of motion of the director will be the same except that φ will be replaced with $\tilde{\varphi} = 2(\vartheta - \psi)$.

When Eq. (3) is investigated in the theory of liquid crystals, it is usually linearized and the inertial term $J(\partial^2\varphi/\partial t^2)$ is discarded because it is assumed that J is determined by molecular quantities and is small ($J \sim 10^{-14}$g/cm). There are as yet no measurements of J.

However, the development of the hydrodynamics of liquid crystals and the very introduction of the director $\mathbf{n}$ characterizing a given liquid crystal presupposes averaging over a physically small volume which nevertheless contains a large number of molecules. It is therefore natural to suppose that the moment J is much larger than the moment of inertia of an individual molecule. The fact that J has not been measured may signify that inertial effects do not appear in linear problems of liquid-crystal dynamics, but it does not signify that such effects will be unimportant in the nonlinear case.

Moreover, it is likely that new nematic liquid crystals containing molecules with greater inertia will be synthesized. In particular, inclusion of inertial effects will be necessary in the case of lyotropic liquid crystals for which nematic order is determined by relatively large clusters containing a large number of molecules.

Equation (3) is conveniently rewritten in terms of dimensionless variables as follows:

$$\frac{\partial^2\varphi}{\partial\tau^2} - \frac{\partial^2\varphi}{\partial\xi^2} + \Gamma\frac{\partial\varphi}{\partial\tau} + \sin\varphi = 0, \tag{4}$$

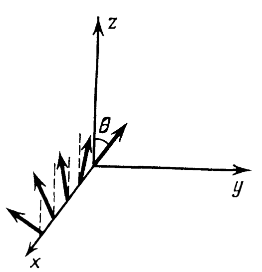

FIG. 1. Pure twist deformation.

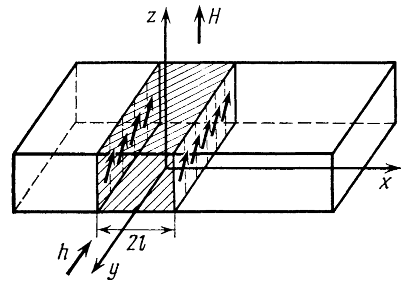

FIG. 2. Geometry of excitation of director motion.

where $\tau = H(\chi_a/J)^{1/2}t$, $\xi = H(\chi_a/K_a)^{1/2}x$, and $\Gamma = \gamma_1/H(\chi_a J)^{1/2}$ is the effective damping.

Generally speaking, the quantity Γ is not small for moderate magnetic fields of $\sim$100–1000 Oe and molecular values of J. However, for fields $\sim 10^4 - 10^5$Oe, $\gamma_1 = 10^{-2}$Pa, and $\chi_a \approx 10^{-6}$ESU, the condition $\Gamma < 1$ can be satisfied for $J \sim 10^{-8}$g/cm. In view of what we have said about the moment of inertia of the director, we shall confine our attention to this particular situation.

Let us now suppose that, at the initial instant of time, a particular region of the specimen is characterized by a rate of deviation of the director from the equilibrium position (determined by the field H) that is uniform in the yz plane (Fig. 2). This could be produced in a variety of ways. For example, it may be produced by a pulsed magnetic or electric field lying in the zy plane at an angle to the z axis, by a hypersonic shock, or by a sudden shift of the surface in this region. The only essential point is that the disturbance must be uniform in the interior of the region, and must have a sharp enough boundary in the x direction. At the next instant of time, the perturbation begins to propagate in the x direction, and the problem is effectively one-dimensional if we neglect the effects of the boundaries of the specimen.

Let us discard the term containing Γ, in (4), i.e., let us ignore, completely dissipation effects to which we shall return later. In this approximation, the problem reduces to an analysis of the equation

$$\frac{\partial^2\varphi}{\partial\tau^2} - \frac{\partial^2\varphi}{\partial\xi^2} + \sin\varphi = 0 \tag{5}$$

subject to the initial conditions

$$\varphi(\xi, 0) = 0, \qquad \frac{\partial\varphi}{\partial\xi}(\xi, 0) = 0, \qquad \frac{\partial\varphi(\xi, 0)}{\partial\tau} = f(\xi).$$

III. SCATTERING MATRIX

To solve this problem, we shall use the inverse scattering method (see Refs. 7 and 8 and the references cited therein), which has undergone intensive development during the last decade. The procedure employed in this method is to find for the initial condition a set of values, the so-called scattering data, then take their transform with respect to the time τ, and, finally, reconstruct the solution of the equation that corresponds to the transformed scattering data. In general, Eq. (5) is the compatibility condition for the set of equations[9,10]

$$\psi_\xi = \frac{i\lambda}{2} U_1\psi + \frac{1}{8i\lambda} U_2\psi + \frac{i}{4} U_3\psi,$$

$$\psi_\tau = -\frac{i\lambda}{2} U_1\psi + \frac{1}{8i\lambda} U_2\psi - \frac{i}{4} U_3\psi,$$

where

$$\psi = \begin{pmatrix} \psi_1 \\ \psi_2 \end{pmatrix},$$

and the matrices U_1, U_2, and U_3 have the form

$$U_1 = \begin{pmatrix} 1 & 0 \\ 0 & -1 \end{pmatrix}, \quad U_2 = \begin{pmatrix} \cos\varphi & -i\sin\varphi \\ i\sin\varphi & -\cos\varphi \end{pmatrix},$$

$$U_3 = \begin{pmatrix} 0 & \varphi_\xi - \varphi_\tau \\ \varphi_\xi - \varphi_\tau & 0 \end{pmatrix}.$$

Equation (5) with the above initial conditions can thus be integrated with the aid of the set of differential equations

$$\psi_{1\xi} = \frac{i}{2}\left(\lambda - \frac{1}{4\lambda}\right)\psi_1 - \frac{i}{4} f(\xi)\psi_2,$$

$$\psi_{2\xi} = -\frac{i}{2}\left(\lambda - \frac{1}{4\lambda}\right)\psi_2 - \frac{i}{4} f(\xi)\psi_1, \tag{6}$$

the solutions of which for $\xi \to -\infty$

$$\psi_1(\xi,\lambda) = 0, \quad \psi_2(\xi,\lambda) = \exp\left[-\frac{i}{2}\left(\lambda - \frac{1}{4\lambda}\right)\xi\right]$$

and for $\xi \to +\infty$

$$\psi_1(\xi,\lambda) = b(\lambda)\exp\left[\frac{i}{2}\left(\lambda - \frac{1}{4\lambda}\right)\xi\right],$$

$$\psi_2(\xi,\lambda) = a(\lambda)\exp\left[-\frac{i}{2}\left(\lambda - \frac{1}{4\lambda}\right)\xi\right]$$

at the initial instant of time determine the components of the scattering matrix viz., the transmission coefficient $A^{-i}(\lambda)$ and the reflection coefficient $r(\lambda) = b(\lambda)/a(\lambda)$. The function $a(\lambda)$ is then analytic in the upper half-plane of λ and $|a(\lambda)|^2 + |b(\lambda)|^2 = 1$ for real λ. Once we know the scattering data $a(\lambda)$, $b(\lambda)$, the zeros λ_n of the function $a(\lambda)$, and the coefficients b_n given by

$$\psi_2(\xi, \lambda_n) = b_n\psi_1(\xi, \lambda_n), \tag{6'}$$

we can determine the nature of the solution of (6) $\varphi(\xi,\tau)$ from their form at the initial time.

The time dependence of the scattering data is defined as follows:

$$a(\lambda,\tau) = a(\lambda,0), \quad b(\lambda,\tau) = b(\lambda,0)\exp\left[-i\left(\lambda + \frac{1}{4\lambda}\right)\tau\right],$$

$$\frac{\partial\lambda_n}{\partial\tau} = 0, \quad b_n(\tau) = b_n(0)\exp\left[-i\left(\lambda_n + \frac{1}{4\lambda_n}\right)\tau\right]. \tag{7}$$

Let

$$f(\xi) = \begin{cases} 2f_0 & \text{for} \quad -l \le \xi \le l, \\ 0 & \text{for} \quad \xi < -l, \quad \xi > l, \end{cases} \tag{8}$$

where $2l$ is the size (in dimensionless units) of the region to which the perturbation was applied.

The choice of this initial condition is dictated by its simplicity, since the more complex geometry $f(\xi)$ would appreciably complicate the calculations without introducing any substantial change into the picture of the phenomenon. Moreover, as we shall see later, this initial condition may correspond to a particular experimental situation.

Substituting (8) in (6), and taking $\Lambda = \lambda - 1/4\lambda$, we find that

$$a(\lambda) = \cos l\Delta - \frac{i\Lambda}{\Delta}\sin l\Delta, \tag{9}$$

$$b(\lambda,0) = -\frac{if_0}{\Delta}\sin l\Delta; \quad \Delta = (\Lambda^2 + f_0^2)^{1/2}.$$

In general, the solution of (6) contains both a continuous spectrum and soliton solutions. Knowledge of the reflection coefficient $r(\lambda)$ for real λ gives the necessary information about the continuous spectrum. The soliton part is characterized by the zeros of $a(\lambda)$ in the complex half-plane $\mathrm{Im}\lambda > 0$, and the restriction of $f(\xi)$ to real values leads to a restriction on the disposition of zeros that ensures that they are symmetric relative to the imaginary axis (i.e., a zero λ_n should be accompanied by a zero $-\lambda_n^*$. Consider the equation that determines the zeros of the function $a(\lambda)$:

$$\mathrm{tg}\, l\Delta = -i\Delta/\Lambda \tag{10}$$

for different values of the variable (Λ). Since, for $\lambda = 1/2\, \rho e^{i\alpha}$,

$$\Lambda = \frac{1}{2}\left[\left(\rho - \frac{1}{\rho}\right)\cos\alpha + i\left(\rho + \frac{1}{\rho}\right)\sin\alpha\right], \tag{11}$$

the values of Λ, corresponding to the roots λ_n and $-\lambda_n^*$ are related by $\Lambda(-\lambda_n^*) = -\Lambda^*(\lambda_n)$ and lie in the upper half-plane.

We shall now show that solutions of (10) in the upper half-plane correspond to purely imaginary Λ. To prove this, consider the behavior of the zeros of $a(\Lambda)$ for different values of f_0. When $f_0 = 0$, we have $a(\Lambda) \equiv 1$ in the entire complex plane. For small f_0, the fact that $a(\Lambda) \to 1$ for $|\Lambda| \to \infty$ in the upper half-plane and $a(\Lambda) \sim 1$ on the entire real axis, ensures that the function $a(\Lambda)$ has no zeros in the upper half-plane. However, since $a(\Lambda)$ is an entire function, it must have zeros in the lower half-plane. Since $a(\Lambda)$ is a continuous function of f_0, its zeros pass into the upper half-plane as f_0 increases. It is clear that, for real $\Lambda \neq 0$, the quantity Δ is also real, and (10) has no solutions. Hence, the zeros of $a(\Lambda)$ can penetrate the upper plane from the lower half-plane only through the point $\Lambda = 0$ (we note that $lf_0 = \pi/2 + \pi k$ when a zero passes through $\Lambda = 0$).

Suppose a zero passes through the point $\Lambda = 0$. By virtue of what we have said about the function $a(\Lambda)$, each zero with $\mathrm{Re}\Lambda_n \neq 0$ should correspond to another zero lying symmetrically relative to the imaginary axis. For a pair of zeros to appear as f_0 increases, a multiple zero must pass through $\Lambda = 0$.

For multiple zeros at the points Λ_n, where $a(\Lambda_n) = 0$, we must also have $a'_\Lambda(\Lambda_n)=0$. From (9) we have

$$a'(\Lambda_n)=(il\Lambda_n-1)\frac{if_0\exp(il\Lambda_n)}{f_0^2+\Lambda_n^2}, \tag{12}$$

and hence $a'(0)\neq 0$.

Consequently, a simple zero occurs at the point $\Lambda=0$ and should remain on the imaginary axis as f_0 increases. Since, in general, for all Λ_n on the imaginary axis with $|\Lambda_n|<\infty$, we have $a'(\Lambda_n)\neq 0$, this means that all the zeros subsequently remain on the imaginary axis.

It is clear from (11) that Λ will be purely imaginary in the following two cases:

(a) for $\rho=1$, i.e., when the zeros λ_n of the function $a(\lambda)$ lie on a semicircle of radius 1/2:

$$\Lambda=i\sin\alpha=it,\quad t\leqslant 1,\quad \lambda_1={}^1/_2e^{i\alpha},\quad \lambda_2={}^1/_2e^{i(\pi-\alpha)};$$

(b) for $\alpha=\pi/2$, when the zeros λ_n lie on the imaginary axis:

$$\Lambda=\frac{i}{2}\left(\rho+\frac{1}{\rho}\right)=it,\quad t>1,\quad \rho_{1,2}=t\pm(t^2-1)^{1/2},\quad \rho_1\rho_2=1,$$

$$\lambda_1=\frac{i\rho_1}{2},\quad \lambda_2=\frac{i\rho_2}{2}=\frac{i}{2\rho_1}.$$

We note that in both cases, the roots λ_n corresponding to a particular Λ appear in pairs. In accordance with general theory,[7] in case (a) this implies the formation of a bound state (a breather), whereas in case (b), a kink and antikink appear and move in opposite directions with equal velocity. This form of the solution is a reflection of the symmetry of the problem about the x axis.

Equation (10), written as a function of t, assumes the form

$$\operatorname{tg} l(f_0^2-t^2)^{1/2}=-(f_0^2-t^2)^{1/2}/t \tag{13}$$

and has positive solutions for $t<f_0$. If we substitute $u=l(f_0^2-t^2)^{1/2}$, we find that (13) reduces to the equation $\sin u=\pm u/f_0l$, which is well known in quantum mechanics. Its graphical solution corresponding to our case is shown in Fig. 3.

It is clear from Fig. 3 that, in view of the foregoing, the solution u_1 appears for $lf_0=\pi/2$. The quantity u_1 increases with increasing lf_0, a new root appears for $lf_0=3\pi/2$, and so on. The total number n of roots is determined by the inequality $\pi N-\pi/2\leqslant lf_0<\pi N+\pi/2$.

The quantities t_n (and, correspondingly, Λ_n) can be expressed in terms of u_n as follows:

$$t_n=f_0[1-(u_n/lf_0)^2]^{1/2}$$

and depend both on the disposition of the roots u_1 and on f_0. Thus, different variants of the solutions may appear, depending on f_0 and lf_0. They include soliton-free solutions, solutions with one or several breathers, a mixture of breathers and king–antikink pairs, and one or several kink-antikink pairs.[1)] These cases will be examined in the next sections.

IV. SOLITON-FREE CASE

As already noted, the solution of (5) contains no solitons at $lf_0<\pi/2$. It is, however, interesting to examine its asymptotic behavior for large times in this case we well. Firstly, the asymptotic behavior of the director dynamics has not been previously considered in the nonlinear approximation. Moreover, knowledge of the behavior of the continuous spectrum will provide us with information on the characteristic times for which soliton solutions, if they exist, appear against the background of the continuous spectrum.

The asymptotic behavior of the solution of the sine-Gordon equation in the soliton-free case was studied in Ref. 11. It was shown there that the amplitude $\varphi(\xi,\tau)$ has the form

$$|\varphi(\xi,\tau)|=\frac{1}{\tau^{1/2}}(1-V^2)^{-1/4}\left(\frac{1}{\pi}\ln|a(\lambda)|\right)^{1/2}, \tag{14}$$

where

$$V=\frac{\xi}{\tau},\quad \lambda=\frac{1}{2}\left[\frac{1-V}{1+V}\right]^{1/2}.$$

Substituting a (λ) from (9) in (14) we obtain

$$|\varphi(\xi,\tau)|=\frac{(1-V^2)^{-1/4}}{(2\pi\tau)^{1/2}} \tag{15}$$

$$\times\left[\ln\left|1-\frac{1-V^2}{1+\eta V^2}\sin^2\left(lf_0\left[\frac{1+\eta V^2}{1-V^2}\right]^{1/2}\right)\right|\right]^{1/2},$$

where $\varphi\sim 1$.

Equation (15) becomes appreciably simpler for positive $n<1$ and $V\lesssim 1$ (which, as we shall see, is typical of the experimental situation). The requirement that $\varphi\sim 1$ determines the characteristic time after which a soliton at the point $\xi=V\tau$ becomes distinguishable against the background of the continuous spectrum:

$$\tau\sim(2\pi)^{-1}(1-V^2)^{1/2}\sin^2[lf_0(1-V^2)^{-1/2}]. \tag{16}$$

V. BREATHER SOLUTIONS

In the case of nonreflecting potentials, for which $b(\lambda)\equiv 0$ at all real λ, the solution of (5) has the form[7]

$$\varphi(\xi,\tau)=-4\arg\det(1+d), \tag{17}$$

where

$$d_{mn}(\xi,\tau)=\frac{c_m}{\lambda_n+\lambda_m}\exp\left[i\left(\lambda_m-\frac{1}{4\lambda_m}\right)\xi-i\left(\lambda_m+\frac{1}{4\lambda_m}\right)\tau\right].$$

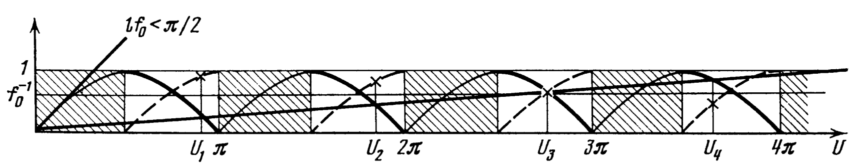

FIG. 3. Graphical solution of (13). There are no soliton solutions in the shaded regions. Dashed lines represents $|\cos U|=t/f_0$. Crosses lying above the f_0^{-1} line correspond to kink-antikink solutions, whereas those below this line correspond to breathers.

Here

$$c_m=\frac{b_m^{(0)}(0)}{a_0'(\lambda_m)},\qquad a_0=\prod_{i=1}^{N}\frac{\lambda-\lambda_i}{\lambda-\lambda_i^*}$$

and $b_m^{(0)}$ correspond to the pure soliton solution.

To take into account the effect of the continuous spectrum on the character of the soliton solutions, let us isolate in the initial scattering data the contribution corresponding to solitons and then, because of the one-to-one correspondence, the soliton solutions will be given by (17) with the parameters determined in this way.

Consider the case where all the roots of (13) are $t_n<1$, i.e., only breathers are produced in the system. Since all the zeros λ_n of the function $a(\lambda)$ lie on a semicircle of radius 1/2, this means that the velocities of all the breathers produced in this way are zero.[7] Because of the symmetry of the problem, their centers lie at the point $\xi=0$. The asymptotic behavior of the solution of (5) for large times τ is shown schematically in Fig. 4a for this case.

Consider the behavior of the solution $\psi_2(\xi,\lambda_n)$ of the set (6), whose asymptotic form as $\xi\to-\infty$ is

$$\psi_2(\xi,\lambda_n)=\exp\left[-\frac{i}{2}\left(\lambda_n-\frac{1}{4\lambda_n}\right)\xi\right].$$

As the region of the continuous spectrum is traversed from left to right up to the region in which the breathers are localized, the function ψ_2 assumes the form

$$\psi_2(\xi,\lambda_n)=A_1(\lambda_n)\exp\left[-\frac{i}{2}\left(\lambda_n-\frac{1}{4\lambda_n}\right)\xi\right],$$

where A_1 is the function $a(\lambda)$ and characterizes the continuous spectrum with wave propagation velocities $V<0$. For a breather corresponding to the roots λ_n and $-\lambda_{n^*}$, the exponential in the last formula represents the asymptotic behavior of the eigenfunction to the left of it, whereas, on the right of it the function ψ_2 assumes the form

$$\psi_2(\xi,\lambda_n)=A_1(\lambda_n)b_n^{(0)}(\tau)\exp\left[\frac{i}{2}\left(\lambda_n-\frac{1}{4\lambda_n}\right)\xi\right]$$

in view of the definition of $b_n^{(0)}$.

On the other hand, if we consider the behavior of the soluton $\psi_1(\xi,\lambda_n)$, that has at $\xi\to+\infty$, the asymptotic form

$$\psi_1(\xi,\lambda_n)=\exp\left[\frac{i}{2}\left(\lambda_n-\frac{1}{4\lambda_n}\right)\xi\right],$$

we should have

$$\psi_1(\xi,\lambda_n)=A_2(\lambda_n)\exp\left[\frac{i}{2}\left(\lambda_n-\frac{1}{4\lambda_n}\right)\xi\right]$$

as we traverse this region from right to left, where $A_2(\lambda_n)$ is the function $a(\lambda)$ and corresponds to a continuous spectrum with wave velocities ($V>0$).

As a result,

$$\psi_2(\xi,\lambda_n)=\frac{A_1(\lambda_n)}{A_2(\lambda_n)}b_n^{(0)}(\tau)\psi_1(\xi,\lambda_n).$$

Comparing this with (6'), we find that

$$b_n^{(0)}(\tau)=\frac{A_2(\lambda_n)}{A_1(\lambda_n)}b_n(\tau). \tag{18}$$

The quantities that we have found refer to the time τ. By referring them to the time $\tau=0$, we obtain precisely those scattering data which describe the soliton solutions with the aid of (17).

Since, by definition, A_1 and A_2 represent the function $a(\lambda)$ for the potential set up by the waves running to the left ($V<0$) and to the right ($V>0$), and the group velocity V is given by

$$V=(4\lambda^2-1)/(4\lambda^2+1),$$

we must have

$$\ln|A_1(\lambda)|=\theta_1(1-4\lambda^2)\ln|a(\lambda)|,$$
$$\ln|A_2(\lambda)|=\theta_2(4\lambda^2-1)\ln|a(\lambda)|,$$

where $\theta(x)=1$ for $x>0$ and $\theta(x)=0$ for $x<0$. Since A_1 and A_2 are analytic for $\mathrm{Im}\lambda>0$, they can be written in the form

$$A_{1,2}(\lambda)=\exp\left[\frac{1}{\pi i}\int_{-\infty}^{\infty}\frac{\ln|A_{1,2}(\lambda')|}{\lambda'-\lambda}d\lambda'\right]$$
$$=\exp\left[\frac{1}{\pi i}\int_{-\infty}^{\infty}\frac{\theta_{1,2}\ln|a(\lambda')|}{\lambda'-\lambda}d\lambda'\right]. \tag{19}$$

Evaluating A_2/A_1 and recognizing that $b_n(\lambda n)\equiv b(\lambda_n)$, we obtain

$$c_m=\mathrm{sign}(\sin u_m)\frac{2e^{-i\Phi_m}\lambda_m\,\mathrm{Im}\,\lambda_m}{\mathrm{Re}\,\lambda_m}$$
$$\times\prod_{i\neq m}^{N}\frac{[1-(u_m/lf_0)^2]^{1/2}+[1-(u_i/lf_0)^2]^{1/2}}{[1-(u_m/lf_0)^2]^{1/2}-[1-(u_i/lf_0)^2]^{1/2}}, \tag{20}$$

where u_j is the root corresponding to the zeros λ_j and λ_j^* (see Fig. 3), N is the number of possible roots u_j,

$$\Phi_m=(2\pi)^{-1}\left[\left(\frac{u_m}{lf_0}\right)^2-\eta\right]^{1/2}$$
$$\times\int_1^{\infty}\frac{\ln(1-w^{-1}\sin^2 lf_0w^{1/2})}{[w-(u_m/lf_0)^2](w-\eta)^{1/2}}dw, \tag{21}$$

and $\eta=(f_0^2-1)f_0^{-2}$.

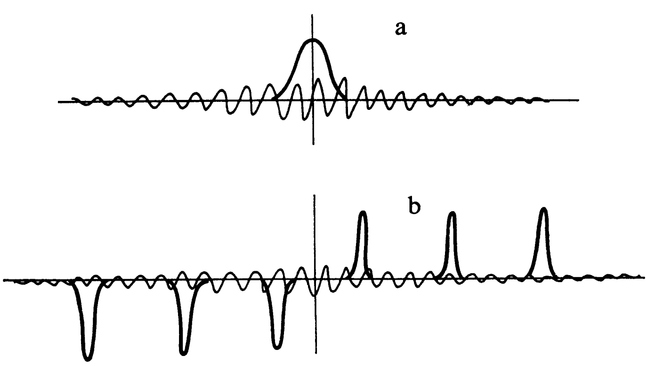

FIG. 4. Schematic representation of the asymptotic form of the solution of (5): (a) the thick line corresponds to a breather and the thin line to the continuous spectrum; (b) the thick line corresponds to $\partial\varphi/\partial\xi$ for kinks and antikinks, and the thin line to the continuous spectrum.

As noted above, substitution of the above expressions for c_m in (17) gives the complete description of the set of N breathers. The solution is quite complicated, so that we shall write out only the explicit form of $\varphi(\xi,\tau)$ for one breather. We then have

$$\varphi=4\,\mathrm{arctg}\left[t(1-t^2)^{-1/2}\frac{\sin(\tau(1-t^2)^{1/2}+\Phi_1)}{\mathrm{ch}\,\xi t}\right];\qquad t=f_0[1-(u_1/lf_0)^2]^{1/2}. \tag{22}$$

It is clear from (22) that the solution is a function that is periodic in time. When t is close to unity, the amplitude of the breather is $\sim 2\pi$, and the localization region is ~ 1.

VI. KINK-ANTIKINK SOLUTIONS

Let us know consider the case where all the roots of (13) are $t_n > 1$, i.e., only king-antikink pairs are produced in the system. By analogy with the preceding section, we now determine the scattering data that characterize each soliton. The asymptotic form of the solution of (5) for large values of time τ is shown schematically in Fig. 4b for this case. Each soliton moves with velocity[7]

$$V_n=(4\lambda_n^2+1)/(4\lambda_n^2-1). \tag{23}$$

(We recall that all the zeros λ_n of the function $a(\lambda)$ lie on the imaginary axis in this case.)

Let us now label all the solitons from left to right with an index k that runs through the values 1 to $2N$, where N is the total number of zeros of the roots of (13). We shall determine the scattering data for the nth soliton moving in the positive direction of ξ with velocity V_n. The solution $\varphi_2(\lambda_n,\xi)$ of (6) which, has the asymptotic form

$$\psi_2=\exp\left[-\frac{i}{2}\left(\lambda_n-\frac{1}{4\lambda_n}\right)\xi\right]$$

as $\xi\to\infty$, takes on the left of the first soliton the form

$$\psi_2=A_1(\lambda_n)\exp\left[-\frac{i}{2}\left(\lambda_n-\frac{1}{4\lambda_n}\right)\xi\right],$$

where A_1 characterizes the continuous spectrum of waves propagating with velocities $V<V_i<0$. As the first soliton passes, ψ_2, which is not its eigenfunction, acquires only the factor $(\lambda_n-\lambda_i)/(\lambda_n-\lambda_i^*)$ (Ref. 7), and so on. Thus, to the left of the nth soliton the function ψ_2 has the form

$$\psi_2=A_1(\lambda_n)\ldots A_n(\lambda_n)\prod_{k=1}^{n-1}\frac{\lambda_n-\lambda_k}{\lambda_n-\lambda_k^*}\exp\left[-\frac{i}{2}\left(\lambda_n-\frac{1}{4\lambda_n}\right)\xi\right].$$

To the right of the nth soliton, ψ_2 has the form

$$\psi_2=A_1(\lambda_n)\ldots A_n(\lambda_n)b_n^{(0)}(\tau)\prod_{k=1}^{n-1}\frac{\lambda_n-\lambda_k}{\lambda_n-\lambda_k^*}\times\exp\left[\frac{i}{2}\left(\lambda_n-\frac{1}{4\lambda_n}\right)\xi\right].$$

By analogy with the foregoing, if we study the behavior of the solution $\psi_i(\lambda_u,\xi)$ which, as $\xi\to+\infty$ the asymptotic form

$$\psi_1(\lambda_n,\xi)=\exp\left[\frac{i}{2}\left(\lambda_n-\frac{1}{4\lambda_n}\right)\xi\right]$$

we finally obtain

$$b_n^{(0)}=\frac{A_>}{A_<}b_n(0)\prod_{k=1}^{n-1}\frac{\lambda_n-\lambda_k^*}{\lambda_n-\lambda_k}\prod_{k=n+1}^{2N}\frac{\lambda_n-\lambda_k}{\lambda_n-\lambda_k^*}. \tag{24}$$

Here $A_>$ and $A_<$ are $a(\lambda)$ for the continuous spectrum propagating with velocities respectively greater than and smaller than V_n. In analogy with (19),

$$A_>=\exp\left[\frac{1}{i\pi}\int_{-\infty}^{\infty}\theta\left(\frac{4\lambda'^2-1}{4\lambda'^2+1}-V_n\right)\ln|a(\lambda')|\frac{d\lambda'}{\lambda'-\lambda}\right],$$

$$A_<=\exp\left[\frac{1}{i\pi}\int_{-\infty}^{\infty}\theta\left(V_n-\frac{4\lambda'^2-1}{4\lambda'^2+1}\right)\ln|a(\lambda')|\frac{d\lambda'}{\lambda'-\lambda}\right]. \tag{25}$$

Substituting in (24) the values of λ_n expressed in terms of the roots of (13) and expressions (25), we finally obtain

$$b_n^{(0)}(0)=-\frac{it_m}{(t_m^2-1)^{1/2}}\prod_{k=1}^{m-1}\frac{(t_k^2-1)^{1/2}-(t_m^2-1)^{1/2}}{(t_k^2-1)^{1/2}+(t_m^2-1)^{1/2}}\prod_{k=m+1}^{N}\frac{t_m+t_k}{t_m-t_k}e^{B_n}, \tag{26}$$

where

$$B_n=\frac{|\lambda_n|}{\pi}\left[\int_{|\lambda_n|}^{\infty}\frac{\ln|a(\lambda)|^2}{\lambda^2+|\lambda_n|^2}d\lambda-\int_0^{|\lambda_n|}\frac{\ln|a(\lambda)|^2}{\lambda^2+|\lambda_n|^2}d\lambda\right], \tag{27}$$

and t_m is the root of (13) corresponding to the nth soliton. If we know $b_n(0)$, we can immediately write down the form of the nth soliton[7]

$$\varphi_n(\xi,\tau)=4\,\mathrm{arctg}\exp\left[-\varepsilon\frac{\xi-\xi_{0n}-V_n\tau}{(1-V_n^2)^{1/2}}\right], \tag{28}$$

$$\xi_{0n}=t_m^{-1}\ln\left|\frac{t_m}{(t_m^2-1)^{1/2}}\times\prod_{k=1}^{m-1}\frac{(t_k^2-1)^{1/2}-(t_m^2-1)^{1/2}}{(t_k^2-1)^{1/2}+(t_m^2-1)^{1/2}}\prod_{k=m+1}^{N}\frac{t_m+t_k}{t_m-t_k}\right|+B_nt_m^{-1},\quad \varepsilon=\mathrm{sign}(2i|\lambda_n|b_n^{(0)}(0)). \tag{29}$$

The sign of ε sets the form of the soliton: a kink occurs for $\varepsilon=-1$ and an antikink for $\varepsilon=1$. The square root in the denominator of (28) determines the characteristic dimensions of the soliton, and ξ_{0n} gives the coordinate of the center of the soliton at the initial time.

It is clear from (13) that the quantities t_m decrease with increasing number of the root. There is a corresponding reduction in the velocities $V_n=t_m^{-1}(t_m^2-1)^{1/2}$. We note, by the way, that the maximum possible soliton velocity in the system is $V_{max}=\eta^{1/2}$, since the maximum value of t_m is f_0 (for $lf_0\to\infty$). Thus, the solution $\varphi(\xi,\tau)$ for $\varphi\,\xi>0$ is a sequence of antikinks with the one on the extreme right propagating with the maximum possible velocity, determined by the first root of (13). It is clear that by virtue of the symmetry of the problem the solution $\varphi(\xi,\tau)$ will be symmetric about $\xi=0$, i.e., an equal number of kinks will be present on the left of the origin. When the solution includes breathers, there is no difficulty in taking into account their effect on the characteristics of the kinks. Considerations similar to those used above can readily be used to show that here again $b_n^{(0)}$ are given by (26), where the $t_k<1$ corresponding to breathers are taken into account in the second product, and N is the total number of roots of (13).

It is interesting to consider the separation $d_{m,m+1}$ between the centers of neighboring solitons (kinks or antikinks) since, as will be shown later, this quantity can readily be observed experimentally. For the mth and $(m+1)$ st solitons, sufficiently large N (i.e., lf_0), and m not too close to N (i.e., for solitons closest to the origin), we can write with good precision (see the Appendix)

$$d_{m,m+1}=\xi_{0m}-\xi_{0m+1}+(V_m-V_{m+1})\tau \approx \frac{2}{f_0}\ln\left[\frac{lf_0}{u_1}\eta^{1/2}\right]+\frac{1-\eta}{\eta}\frac{u_1u_m}{(lf_0)^2}\tau. \quad (30)$$

Since $u_m\sim mu_1\sim m\pi$ and $lf_0\sim N\pi$, it is clear that for

$$\tau\lesssim\frac{2\eta^{1/2}N}{\pi m}\ln(N\eta^{1/2})$$

the separation $d_{m,m+1}$ remains practically unaltered and is determined by the initial parameter of the problem. For large times, the separation between the solitons increases linearly with time. The ratio of the characteristic soliton size $(1-V_m^{\,2})^{1/2}=t_m^{\,-1}$ to the separation between neighboring solitons characterizes the degree of overlap of the soliton solutions.

For $\eta\lesssim 1$, we find from that

$$t_m^{-1}/d_{m,m+1}<[2\ln(\eta^{1/2}N)]^{-1}\ll 1.$$

This means that solitons are well separated in space and may be looked upon as independent.

Finally, consider the effect of the dissipative term $\Gamma(\partial\varphi/\partial\tau)$ on the form of the solution of (4). No solution of (4) can be found for arbitrary Γ. When $\Gamma\ll 1$, the soliton solution can be found with the help of perturbation theory[12] and has the following form in a coordinate frame moving with the soliton velocity:

$$\varphi(\xi,\tau)=\varphi_c+\varphi_b,$$

where φ_c is the solution obtained previously without dissipation and

$$\varphi_b=V_n\left[\tau-\left(1-\exp\left(-\frac{\Gamma\tau}{(1-V_n^{\,2})^{1/2}}\right)\right)\Big/\Gamma(1-V_n^{\,2})^{1/2}\right]\times\operatorname{sech}\xi.$$

This means that the solution of (4) will have the form of solitons propagating with the same velocities as in the absence of damping, but their shape will depend on time (the soliton amplitude will decrease and they will expand).

VI. DISCUSSION OF RESULTS AND OF POSSIBLE EXPERIMENTAL VERIFICATION

Consider a possible experiment in which the initial data of the above problem can be implemented. Suppose that a nematic liquid crystal is placed in a constant magnetic field **H** perpendicular to the crystal layer at time $t=0$ and a magnetic field pulse $\mathbf{h}\perp\mathbf{H}$ is applied to the region $2l$, as shown in Fig. 2. Using the same assumptions about the characteristic parameters and the damping γ_1 as above, we find that the equation of the director motion can be written in the form

$$J\ddot{\varphi}+\chi_a(H^2-h^2)\sin\varphi-2hH\cos\varphi=0. \quad (31)$$

The gradient terms in (4) have been discarded here because, by virtue of the homogeneity of the conditions, they will be appreciable only on the boundaries of the region to which the field is applied and will have little effect on the final result for sufficiently short pulses.

The initial data that could correspond to the above problem are: the quantity φ must remain small for $(\varphi\ll 1)$ during the time t_p of application of the magnetic-field pulse, whereas the rate of rotation of the director φ must assume an appreciable value.

For small φ, Eq. (31) can be linearized and its solution corresponding to $h>H$ has the form[2)]

$$\varphi=\frac{hH}{h^2-H^2}\operatorname{sh}^2\left(\frac{\Omega t}{2}\right),\qquad \Omega=\left(\frac{h^2-H^2}{J}\chi_a\right)^{1/2}.$$

Substituting $h=\alpha H$, we find that, when

$$\operatorname{sh}\left(\frac{\Omega t_p}{2}\right)\ll\left(\frac{\alpha^2-1}{4\alpha}\right)^{1/2} \quad (32)$$

we have $\varphi\ll 1$.

In terms of the dimensionless variables introduced in Sec. 2,

$$\frac{\partial\varphi}{\partial\tau}=2\alpha(\alpha^2-1)^{-1/2}\operatorname{sh}\Omega t_p.$$

When α is not too large, condition (32) yields $t_p\sim\Omega^{-1}$, so that $\partial\varphi/\partial\tau\sim 1$. For example, for $\alpha=10$ and $\Omega t_p=1$, we obtain $\varphi\approx 0.1$ and $\partial\varphi/\partial\tau=2f_0=2.4$. The corresponding pulse length is of the order of 10^{-6} s.

Thus, the quantity f in the expressions obtained in the preceding sections will be of the order of unity in the region accessible to experimental examination.

The consequence of this result is that the necessary condition for the appearance of a sufficiently large number N of solitons is that $l\sim N\pi/2f_0$ be large. The velocities of solitons with numbers not too close to N will be $V_n\lesssim\eta^{1/2}<1$, where $n\lesssim 1$, i.e., this justifies the assumption made in the derivation of (16) and (30).

The characteristic time after which the amplitude of the continuous spectrum becomes much smaller than the amplitude of the soliton solutions is seen from (15) to have the largest value for $V=0$, i.e., at the origin, where it is given by

$$\tau_{max}=(2\pi)^{-1}\ln(\cos lf_0).$$

For solitons propagating with velocities $V_n \sim \eta^{1/2}$, condition (15), which takes the form

$$|\varphi(\xi,\tau)| = \left(\frac{\eta^{1/2} f_0}{2\pi\xi}\right)^{1/2} \left(\ln \left|1 - \frac{\sin^2 l f_0 (1+\eta)^{1/2}}{1+\eta}\right|\right)^{1/2}$$

is well satisfied for ξ greater than $\eta^{1/2} f_0/2\pi$.

As an example, consider the characteristic soliton parameters in the specific case where $f_0 = 1$ and 2, $N = 20$ in terms of dimensional variables with the indicated $H\chi_a$, and J, and $K_2 \sim 10^{-6}$ dyn. For these parameters, $l = 10^{-2}$ cm, $\eta = 0.3$, $V_{1,2,3,4} = 5.5$, 5.3, 4.9, and 4.1 cm/s, respectively, $\tau_{\max} \sim 10^{-5}$ s, and $d_{1,2} = 10^{-3}$ cm. The characteristic dimension of the first few solitons is then about 3×10^{-4} cm, and the distance from the origin for which the time dependence in $d_{m,m+1}$ becomes important is about 10^{-2} cm. As time increases, the separation between neighboring solitons will also increase and, after an interval of the order of a second, it will reach a few millimeters, by which time the solitons themselves will have traversed a few centimeters.

The foregoing estimates show that the situation described above can definitely be attained under reasonable experimental conditions. The simplest approach to an experimental verification of these results is to use optical methods.[13]

The tilt θ of the director from the equilibrium position in the above solution should take the form of a moving alternation of bands with $\theta \simeq 0$, and much narrower bands corresponding to kinks and antikinks within which the angle θ varies from zero to π. (The fact that the successive kinks or antikinks differ in amplitude by 2π has no effect on the result because this simply indicates a rotation of the director through the angle π, i.e., into an identical state.) When breathers are present, the neighborhood of the origin will contain a region in which the tilt of the director from the equilibrium position varies with time in a rather complicated manner, and the amplitude of the variation is determined by its value for the highest breather.

If we place the specimen between two crossed polarizers, oriented at 45° to the direction of propagation of the solitons, and observe the transmission of natural light in the direction perpendicular to the surface of the specimen, we should observe at a fixed instant of time a sequence of dark and bright bands. Light bands correspond to solitons and their centers coincide with the coordinates of the soliton centers, where $\theta = \pi/2$. By observing these bands, we should be able to determine the speed of the solitons, their number as a function of the exciting fields strengths, and the characteristic dimensions of the solitons.

CONCLUSION

Our analysis has shown that soliton solutions for the motion of the director in a magnetic field are possible in nematic liquid crystals when the characteristic parameters of the specimen satisfy certain conditions. Experimental studies of these phenomena would be useful because they would provide information about the magnitude of the moment of inertia J.

Although the excitation producing the motion of the director was assumed to be a pulsed magnetic field, the results can readily be extended to other cases. A modified version of the above method can be used to examine the motion of the director in an electric field, as well as a number of other problems that lead to the Sine-Gordon equation.

The authors are indebted to E. I. Kats and S. V. Manakov for numerous useful discussions.

APPENDIX

Let us write ξ_{0n} [Eq. (29)] in the form $\xi_{0n} = \tilde{\xi}_{0n} + B_n t_m^{-1}$, and first estimate $\tilde{\xi}_{0n}$ for a sufficiently large N (i.e., lf_0) and for the antikink numbered m not too close to N. Under these assumptions, $u_m (lf_0)^{-1} \approx m/N < 1$ because $u_m (lf_0)^{-1} \sim 1$ only for the last root of (13). The presence of breathers in the system improves the situation, since we then have $u_m (lf_0)^{-1} \approx (N-n)/N < 1$, where n is the total number of breathers in the system, even for the last of the possible antikinks. Thus, assuming that $u_m (lf_0)^{-1} \ll 1$ and η is not too small in comparison with unity, we find that

$$t_m \approx f_0[1 - u_m^2 (lf_0)^{-2}/2],$$
$$(t_m^2 - 1)^{1/2} \approx f_0 \eta^{1/2} [1 - u_m^2 (lf_0)^{-2}/2\eta]. \tag{A.1}$$

Substituting these values in the expression for $\tilde{\xi}_{0n}$, and recalling that for large N and $m \ll N$ we may write with sufficient precision $u_m \approx m u_i$, we find that

$$\tilde{\xi}_{0n} = t_m^{-1} \ln \left\{ \eta^{1/2} \left[\frac{4\eta (lf_0)^2}{u_1^2}\right]^{N-n-2m+1} \prod_{k=1}^{m-1} (m^2 - k^2) \times \prod_{k=m+1}^{N-n} (k^2 - m^2)^{-1} \times \prod_{k=N-n+1}^{N} \frac{t_m + t_k}{t_m - t_k} \right\} = t_m^{-1} \ln \left\{ \eta^{1/2} \left[\frac{4\eta (lf_0)^2}{u_1^2}\right]^{N-n-2m+1} \times \frac{(2m-1)!(2m)!}{m(N-n-m)!(N-n+m)!} \prod_{k=N-n+1}^{N} \frac{t_m + t_k}{t_m - t_k} \right\}: \tag{A.2}$$

The contribution due to breathers has been taken into account in the last product. Writing out the analogous expression for the $n+1$ st antikink, and subtracting one from the other, we obtain

$$\tilde{\xi}_{0n} - \tilde{\xi}_{0n+1} = t_m^{-1} \left\{ 2 \ln \left[\frac{\eta (2lf_0)^2}{u_1^2}\right] + \ln \frac{N-n+m+1}{4m^2 (2m+1)^2 (N-n-m)} + \ln \prod_{k=N-n+1}^{N} \frac{t_m^2 - t_k^2 - \gamma t_m t_k}{t_m^2 - t_k^2 + \gamma t_m t_k} \right\}, \tag{A.3}$$

where $\gamma = t_m t_{m+1}^{-1} - 1 \ll 1$.

It is clear that, under the above assumptions about the values of N and m, and provided that the number n of breathers is not large in comparison with N, the leading term in

(A.3) is the first logarithm, i.e.,

$$\xi_{0n}-\xi_{0n+1}\approx 2f_0^{-1}\ln\,[\eta(2lf_0)^2/u_1^2]. \qquad \text{(A.4)}$$

Let us now estimate the difference $B_n t_m^{-1} - B_{n+1} t_{m+1}^{-1} = \tilde{B}$.. Since $\lambda_n = t_m + (t_2^m - 1)^{1/2}$ and λ_{n+1} are not very different, we have

$$\tilde{B}\approx\pi^{-1}(\lambda_n-\lambda_{n+1})\frac{d}{d\lambda_n}\left[\int\limits_1^\infty\frac{\ln|a(\lambda_n t)|^2\,dt}{t^2+1}-\int\limits_0^1\frac{\ln|a(\lambda_n t)|^2\,dt}{t^2+1}\right]. \qquad \text{(A.5)}$$

Differentiating under the integral sign and evaluating the integrals, we obtain

$$\tilde{B}\approx\frac{1}{\pi}(\lambda_n-\lambda_{n+1})\left\{-\ln\left[1-\frac{\sin^2 lf_0(1+\eta)^{1/2}}{1+\eta}\right]\right.$$
$$\left.+\int\limits_1^\infty\frac{t^2-1}{(t^2+1)^2}\ln|a(\lambda_n t)|^2\,dt-\int\limits_0^1\frac{t^2-1}{(t^2+1)^2}\ln|a(\lambda_n t)|^2\,dt\right\}.$$

We now make the change of variable $t\to l/t$ in the last integral and recognize that $a(\lambda_n/t)=a(t/\lambda_n)$, as can be readily verified. We thus obtain

$$\tilde{B}\approx\frac{1}{\pi}(\lambda_n-\lambda_{n+1})\left\{-\ln\left[1-\frac{\sin^2 lf_0(1+\eta)^{1/2}}{1+\eta}\right]\right.$$
$$\left.+\int\limits_1^\infty\frac{t^2-1}{(t^2+1)^2}[\ln|a(\lambda_n t)|^2-\ln|a(t/\lambda_n)|^2]dt\right\}.$$

Since, moreover, for $\eta\lesssim 1$ both λ_n and λ_n^{-1} are close to unity, we have

$$\tilde{B}\approx\frac{1}{\pi}(\lambda_n-\lambda_{n+1})\left\{-\ln\left[1-\frac{\sin^2 lf_0(1+\eta)^{1/2}}{1+\eta}\right]\right.$$
$$\left.+(\lambda_n-\lambda_n^{-1})\frac{d}{d\lambda_n}\int\limits_1^\infty\frac{t^2-1}{(t^2+1)^2}\ln|a(\lambda_n t)|^2\,dt\right\}. \qquad \text{(A.6)}$$

Integration in this expresison leads to a rapidly converging integral $I<1$ multiplied by the small quantity $\lambda_n-\lambda_n^{-1}$, so that the first term in the braces is, in fact, the leading term. We thus finally obtain

$$\tilde{B}\approx-\frac{mu_1^2}{4\pi(lf_0)^2}\ln\left[1-\frac{\sin^2 lf_0(1+\eta)^{1/2}}{1+\eta}\right]\sim\frac{m}{N^2}. \qquad \text{(A.7)}$$

Comparison of (A.7) with (A.4) yields ultimately (30).

[1)]For $f_0<1$, the only soliton solutions are breathers.
[2)]The case $h<H$ corresponds to $f_0<0$ and leads only to breather solutions.

[1]P. G. De Gennes, The Physics of Liquid Crystals, Oxford University Press, 1974 [Russian transl., Mir, Moscow, 1977].
[2]S. Chandrasekhar, Liquid Crystals, Cambridge Univ. Press, 1977. [Russian transl., Mir, Moscow, 1980].
[3]V. L. Golo, E. I. Kats, and A. A. Leman, Zh. Eksp. Teor. Fiz. **86**, 147 (1984) [Sov. Phys. JETP **59**, 84 (1984)].
[4]Zhu Guozhen, Phys. Rev. Lett. **49**, 1332 (1982).
[5]Lin Lei, Shu Changqing, Shen Juelian, et al., Phys. Rev. Lett. **49**, 1335 (1982).
[6]J. L. Ericksen, Phys. Fluids **9**, 1205 (1966); F. M. Leslie, Quart. J. Mech, Appl. Math. **19**, 357 (1966).
[7]V. E. Zakharov, S. V. Manakov, S. P. Novikov, and L. P. Pitaevskiĭ, Teoriya solitonov (Theory of Solitons), Nauka, Moscow, 1980.
[8]M. Ablowitz and H. Segur, Solitons and the Inverse Scattering Transform, SIAM, Philadelphia, 1981.
[9]V. E. Zakharov, L. A. Takhradzhyan, and L. D. Fadeev, Dokl. Akad. Nauk SSSR **219**, 6 (1974) [Sov. Phys. Dokl. **19**, 824 (1975)].
[10]M. J. Ablowitz, D. J. Kaup, A. C. Newell, and H. Segur, Phys. Rev. Lett. **30**, 1262 (1973).
[11]V. E. Zakharov and S. V. Manakov, Zh. Eksp. Teor. Fiz. **71**, 203 (1976) [Sov. Phys. JETP **44**, 106 (1977)].
[12]M. Fogel, S. Trullinger, and A. Bishop, Phys. Rev. B **15**, 1578 (1977).
[13]L. M. Blinov, Elektro-i magnitooptika zhidkikh kristallov (Electro- and Magnetooptics of Liquid Crystals), Nauka, Moscow, 1978.

Translated by S. Chomet